Short communication

The destabilization mechanism and de/re-hydrogenation kinetics of MgH₂–LiAlH₄ hydrogen storage system

Yao Zhang [a,*], Qi-Feng Tian [b,c], Shu-Sheng Liu [a], Li-Xian Sun [a]

[a] *Materials and Thermochemistry Group, Dalian Institute of Chemical Physics, Chinese Academy of Sciences, Dalian, Liaoning 116023, China*
[b] *Key Laboratory for Green Chemical Process of Ministry of Education, Wuhan Institute of Technology, Wuhan 430073, China*
[c] *Hubei Key Laboratory of Novel Reactor & Green Chemical Technology, Wuhan Institute of Technology, Wuhan 430073, China*

A B S T R A C T

Unfavourable stability and sluggish de/re-hydrogenation kinetics hamper the application of MgH₂ as a hydrogen storage material for mobile fuel cell systems. In the present work, it can be destabilized effectively by LiAlH₄ in as-synthesized MgH₂–LiAlH₄ composites (1:1, 2:1 and 4:1 in mole ratio). The onset dehydrogenation temperature of MgH₂ is observed at around 250 °C, which is over 50 °C lower from that of as-milled MgH₂. Differential scanning calorimetry (DSC) measurements indicate that the enthalpies of MgH₂-relevant decomposition in MgH₂–LiAlH₄ composites (1:1, 2:1 and 4:1 in mole ratio) are 45, 48.6 and 61 kJ mol⁻¹ H₂, respectively. These values decrease significantly from that of as-milled pristine MgH₂ (76 kJ mol⁻¹ H₂), demonstrating the destabilization of MgH₂ in this system. The destabilization mechanism is investigated by X-ray diffraction (XRD) analyses. It was found that the whole dehydrogenation process can be divided into two stages: the first stage is the two-step decomposition of LiAlH₄ and during the second stage, the yielded LiH and Al phases decompose MgH₂ to form Li₀.₉₂Mg₄.₀₈ and Mg₁₇Al₁₂ phases, respectively. The mutual destabilization between MgH₂ and LiH was first observed in this study. Moreover, the reaction is fully reversible. The isothermal kinetics shows that the doped LiAlH₄ is beneficial to the enhancement of the dehydrogenation kinetics of MgH₂.

© 2008 Elsevier B.V. All rights reserved.

1. Introduction

Large volumetric (>62 kg m⁻³) and gravimetric (>6.5 wt.%) densities are strictly desired for on-board hydrogen storage in fuel cell vehicles according to the U.S. DOE's 2010 target [1,2]. Magnesium hydride possessing large gravimetric density (7.6 wt.% H₂), abundant resources and low cost can sufficiently meet the requirements of application. Nevertheless, MgH₂ still suffers from both unfavorable thermal stability (76 kJ mol⁻¹ H₂) and sluggish de/re-hydrogenation kinetics. It requires ~300 °C to dehydrogenate over 0.1 MPa. During recent years, many approaches have been tried to improve its hydrogen storage properties, for instance, preparing nano-crystalline MgH₂ produced by high energy milling [3], or doping some catalysts such as metals [4–8], alloys [9,10], metal oxides [11–16] and metal halides [17–23], etc.

However, the above efforts merely enhanced its kinetic performances. The thermodynamic characteristics of the interaction between Mg and hydrogen are hardly influenced. From this point,

Vajo tried to destabilize MgH₂ using some elements such as Si [24]. It was observed that the formation of an intermediate phase such as Mg₂Si is beneficial to MgH₂ destabilization. Nevertheless, the Si-doped system would inevitably reduce the gravimetric hydrogen density because Si does not hydrogenate. Moreover, it seems hardly reversible. In the present work, we suggest a way to destabilize MgH₂ using a complex hydride with a high gravimetric density such as LiAlH₄. This idea is based on the hypothesis that so-called mechano-chemical reactions could occur between MgH₂ and LiAlH₄, and that some intermediate phases could be formed to tailor the thermal stability. However, its unclear for the reaction pathways in the composite system. Therefore, its necessary to reveal which mechanism definitely works in this system, and whether MgH₂ could directly react with LiAlH₄ or with the yielded phases of LiAlH₄ decomposition. The de/re-hydrogenation kinetics will also be investigated in this work.

2. Experimental

The commercial MgH₂ (98%, Alfa Aesar), LiAlH₄ (97%, Alfa Aesar) and their mixtures (in mole ratio of 1:1, 2:1 and 4:1) were ground upon a QM-1SP planetary ball mill for 1 h at the rate of 450 rpm.

* Corresponding author. Tel.: +86 411 84379215; fax: +86 411 84379215.
E-mail address: zhangyao@dicp.ac.cn (Y. Zhang).

In each stainless milling pot (100 ml), the ball-to-powder weight ratio was 50:1 and the protection atmosphere was 0.1 MPa Ar. All handling of the samples were conducted in an MBraun Unilab glove box filled with high-purity Ar (99.9999%) and low-concentration H_2O (<0.1 ppm) and O_2 (<0.1 ppm).
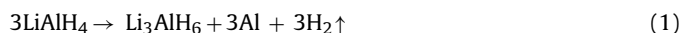
Non-isothermal dehydrogenation performances were investigated by thermogravimetry (TG) and differential scanning calorimetry (DSC). The experiments of TG were executed upon a TherMax 500 (Thermo Cahn). A sample of approximately 2 mg was tested by DSC (SETARAM DSC141) using 0.1 MPa of helium with a purge rate of 50 ml min^{-1}. All these measurements were performed at a heating rate of 10 °C min^{-1}.

The isothermal de/re-hydrogenation kinetics were measured by a Sieverts-type apparatus (Advanced Materials Corporation) within the pressure range of 0–10 MPa H_2. X-ray diffraction (XRD) measurements upon a PANalytical X'pert diffractometer (Cu Kα, 50 kV, 200 mA) were used to determine the phases in the samples at various states. An amorphous polymer film was used to shield the sample from air when it was tested. Its background was subtracted from the XRD patterns of the present work.

3. Results and discussion

3.1. Reactions in the MgH$_2$–LiAlH$_4$ system

Fig. 1 exhibits the non-isothermal dehydrogenation performances of as-milled MgH$_2$, LiAlH$_4$ and MgH$_2$–LiAlH$_4$ composites tested by TG measurements. The total dehydrogenation amount for MgH$_2$–LiAlH$_4$ samples attain more than 7.0 wt.% H$_2$. We found that there are two significant stages of dehydrogenation occurring during the heating process. The first stage within the temperature range from 100 to 250 °C seems to be the two-step decomposition of as-milled LiAlH$_4$ as indicated in Eqs. (1) and (2), because both dehydrogenation temperatures and hydrogen liberation amounts correspond to the decompositions of LiAlH$_4$ and Li$_3$AlH$_6$ [25], respectively:

$$3LiAlH_4 \rightarrow Li_3AlH_6 + 3Al + 3H_2\uparrow \qquad (1)$$

$$Li_3AlH_6 \rightarrow 3LiH + Al + 3/2H_2\uparrow \qquad (2)$$

In this figure, one finds also that the ball milled LiAlH$_4$ hardly changes its dehydrogenation performance (stages and amount of hydrogen liberation) from that of the as-received one, although its dehydrogenation temperature slightly decreases (around 5 °C)
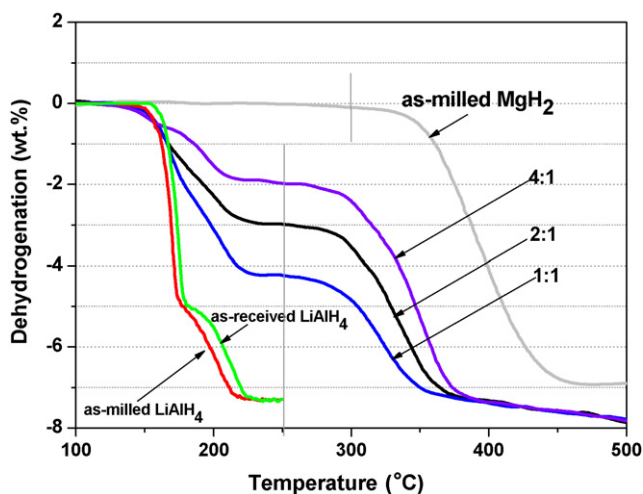

Fig. 1. TG profiles for as-milled pristine LiAlH$_4$ and MgH$_2$, and MgH$_2$–LiAlH$_4$ composites (in mole ratio of 1:1, 2:1 and 4:1), with a heating rate of 10 °C min^{-1}.
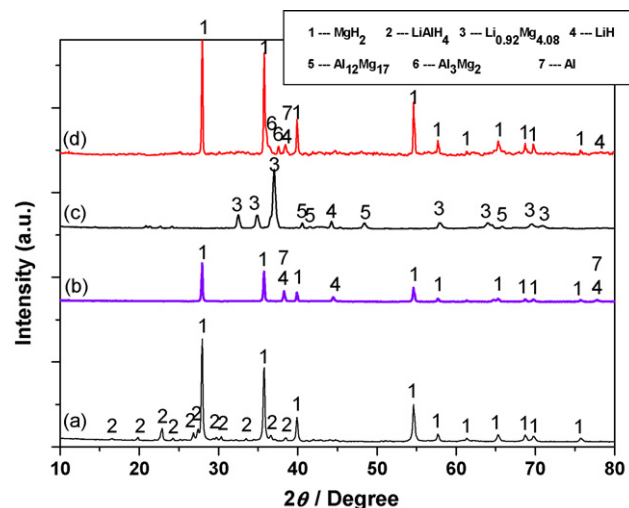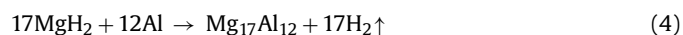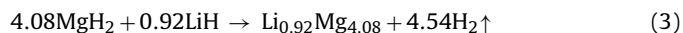

Fig. 2. XRD patterns for the MgH$_2$–LiAlH$_4$ (4:1) composite at different states: (a) before dehydrogenation; (b) after dehydrogenation at 250 °C; (c) after dehydrogenation at 500 °C; (d) after re-hydrogenation at 400 °C.

from the latter because of the activation. The ball milled MgH$_2$ is fully activated on the surface and easily desorbs hydrogen at around 300 °C, which is significantly decreased by 100 °C from those as-received MgH$_2$.

Fig. 2(b) characterizes LiH and Al phases in the XRD pattern of the MgH$_2$–LiAlH$_4$ (4:1) composite after dehydrogenation at 250 °C. It excludes the possibility of MgH$_2$-relevant reactions, demonstrating that only self-decomposition of LiAlH$_4$ dominates this stage.

The second dehydrogenation stage can be ascribed to the MgH$_2$-relevant decomposition according to the estimation of the hydrogen liberation amount at this stage. Primary investigation through TG measurements revealed that the onset temperature of MgH$_2$-relevant decomposition is reduced significantly by 50 °C from as-milled pristine MgH$_2$ (∼300 °C). To study the reaction mechanism working at this stage, the XRD measurements were performed on the MgH$_2$–LiAlH$_4$ (4:1) sample after dehydrogenation at 500 °C. The XRD pattern of Fig. 2(c) suggests that the intermediate phases Li$_{0.92}$Mg$_{4.08}$ and Mg$_{17}$Al$_{12}$ were eventually formed in the composite system at this stage. It indicates that the following reactions must take place within the temperature range from 250 to 500 °C:

$$4.08MgH_2 + 0.92LiH \rightarrow Li_{0.92}Mg_{4.08} + 4.54H_2\uparrow \qquad (3)$$

$$17MgH_2 + 12Al \rightarrow Mg_{17}Al_{12} + 17H_2\uparrow \qquad (4)$$

The inset in Fig. 3 is an endothermic peak corresponding to the second dehydrogenation event of the MgH$_2$–LiAlH$_4$ (1:1) composite. By means of an automatic calibration of the Data Processing Module^{TM} for SETERAM DSC 141, we obtained the onset (314.2 °C), top (334.3 °C) and offset (349.2° C) points of this peak. The reaction enthalpy was also integrated as 674.19 J g^{-1} (hydrides). According to the TG performance of MgH$_2$–LiAlH$_4$ (1:1) composite in Fig. 1, we observed that the dehydrogenation capacity (H/M in weight ratio) of the second stage is about 3.0 wt.%. This means that the hydrogen desorption enthalpy can be calculated as 45 kJ mol^{-1} H$_2$.

By means of the same methods, the reaction enthalpies of other MgH$_2$-relevant decompositions are determined to be 48.6 and 61 kJ mol^{-1} H$_2$ for the MgH$_2$–LiAlH$_4$ composites (2:1 and 4:1 in mole ratio), respectively. These values are significantly smaller than the dehydrogenation enthalpy of as-milled pristine MgH$_2$ (76 kJ mol^{-1} H$_2$), which verifies the destabilization of MgH$_2$ by LiH and Al, respectively.
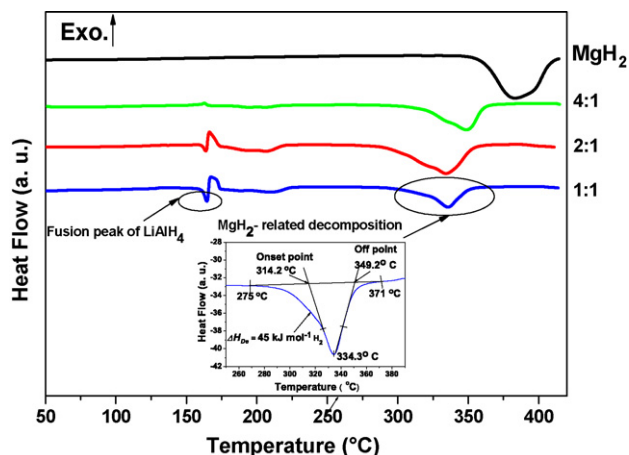
Fig. 3. Differential scanning calorimetric (DSC) traces for as-milled pristine MgH$_2$ and MgH$_2$–LiAlH$_4$ composites (in mole ratio of 1:1, 2:1 and 4:1), with a heating rate of 10 °C min^{-1}.

Fig. 4. TG profiles for as-milled pristine MgH$_2$, MgH$_2$–Al (1:1), MgH$_2$–LiH (1:1), MgH$_2$–LiH–Al (1:1:1) and MgH$_2$–LiAlH$_4$ (1:1), with a heating rate of 10 °C min^{-1}.

Within the composite, the reaction between MgH$_2$ and LiH coincides well with the following equation suggested by Vajo et al. [24]:

$$nAH_x + mBH_y \leftrightarrow A_nB_m + 1/2(nx+my)H_2 \tag{5}$$
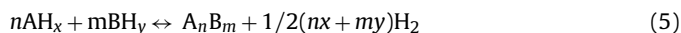
where AH$_x$ and BH$_y$ are binary or more complex hydrides, and n and m are specified by the stoichiometry of the AB alloy. However, the mutual destabilization between two hydrides has not been mentioned in their work. In this case, we observed that the intermetallic alloy Li$_{0.92}$Mg$_{4.08}$ effectively decomposed the strong bonds of Mg–H and Li–H, and destabilized both hydrides simultaneously. Such a reaction exhibits a novel destabilization approach for highly bound hydrides, for example ionic IA and IIA metal hydrides.

On the other hand, aluminum could destabilize MgH$_2$ through forming Mg–Al alloy as previously studied by Zaluska et al. [26]. The yielded γ-Mg$_{17}$Al$_{12}$ phase has already become one example of tailoring a hydride system with high stability.

Fig. 2(d) presents the XRD pattern of the MgH$_2$–LiAlH$_4$ (4:1) composite after re-hydrogenation at 400 °C and under 4 MPa. The yielded LiH and MgH$_2$ phases confirm that the reaction (4) can be conducted in a converse direction as follows:

$$Li_{0.92}Mg_{4.08} + 4.54H_2 \rightarrow 4.08MgH_2 + 0.92LiH \tag{6}$$

It also suggests that Mg$_{17}$Al$_{12}$ can be dissociated into Mg$_2$Al$_3$, MgH$_2$ and Al. This phenomenon coincides with that described by Kuji and Yabe [27], and Zhang and Wu [28], where

$$Mg_{17}Al_{12} + (17-2y)H_2 \rightarrow yMg_2Al_3 + (17-2y)MgH_2 + (12-3y)Al \tag{7}$$
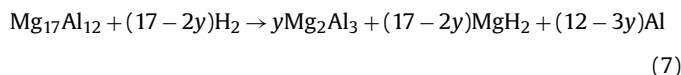
However, Mg$_2$Al$_3$ hardly transforms into MgH$_2$ and Al at the present conditions as shown in (8).

$$Mg_2Al_3 + 2H_2 \rightarrow 2MgH_2 + 3Al \tag{8}$$

Therefore, the reversible hydrogen storage capacity should be reduced because of the formation of the stable phase Mg$_2$Al$_3$. Furthermore, no evidence shows that LiAlH$_4$ or Li$_3$AlH$_6$ could be recovered in this case. It is hereby concluded that only MgH$_2$ is reversible in the composite system because it can be partially recovered.
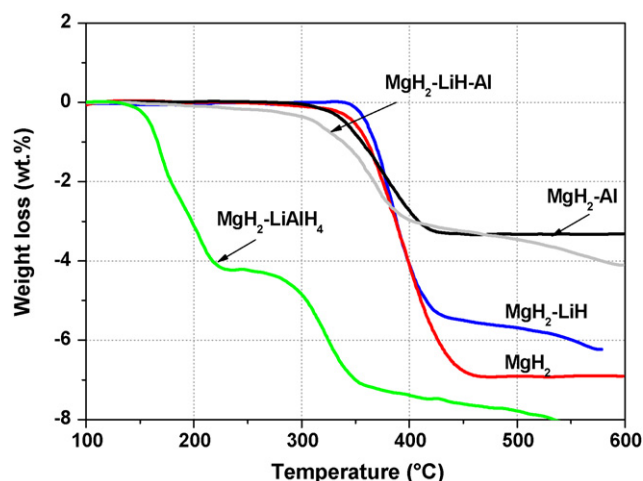
3.2. Reactions in the MgH$_2$–LiH, MgH$_2$–Al and MgH$_2$–LiH–Al systems

The performances of LiH and Al in the MgH$_2$–LiAlH$_4$ composite stimulated our interest to investigate further the MgH$_2$–LiH, MgH$_2$–Al and even MgH$_2$–LiH–Al composites. We exhibit the TG performances of the latter composites in Fig. 4. It indicates that either MgH$_2$–LiH (1:1) or MgH$_2$–Al (1:1) sample can hardly decrease the onset dehydrogenation temperature from that of as-milled pristine MgH$_2$. Their non-isothermal dehydrogenation performances are not as significant as that in the MgH$_2$–LiAlH$_4$ composite. We ascribe this phenomenon to kinetics issues. The possible reason is that LiAlH$_4$ would melt before self-decomposition [29] as the endothermic peak shown in Fig. 3. The subsequently precipitated LiH and Al particles might achieve much higher dispersion on the surface of MgH$_2$ and more compact phase segregation than as-milled MgH$_2$–LiH or MgH$_2$–Al samples. It likely leads to enhanced dehydrogenation kinetics. It was also found that MgH$_2$–LiH–Al (1:1:1) exhibits a decreased dehydrogenation temperature, suggesting that the synergistic work of Al and LiH leads to a more significant effect than that of either LiH or Al alone.

In Fig. 5, the XRD pattern verifies that the Mg$_{17}$Al$_{12}$ is the only product phase in the MgH$_2$–Al composite, which is the same Mg–Al
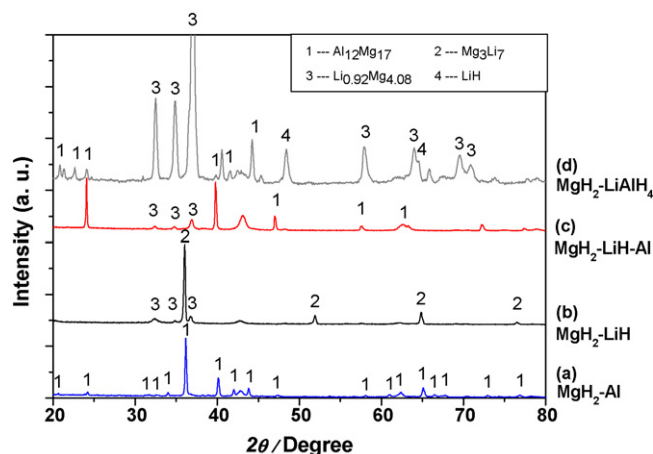
Fig. 5. XRD patterns for (a) MgH$_2$–Al (1:1), (b) MgH$_2$–LiH (1:1), (c) MgH$_2$–LiH–Al (1:1:1) and MgH$_2$–LiAlH$_4$ (1:1) composites after dehydrogenation at 500 °C.
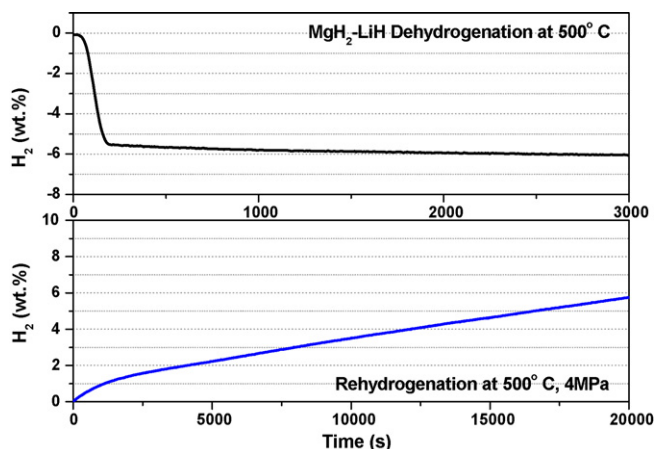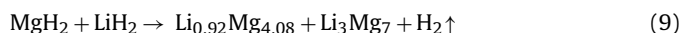
Fig. 6. Isothermal de/re-hydrogenation kinetics for the MgH$_2$–LiH composite (in mole ratio of 1:1) at 500 °C.

phase as yielded in the dehydrogenated MgH$_2$–LiAlH$_4$ system. As for the MgH$_2$–LiH composite, the Mg–Li phases are Li$_3$Mg$_7$ and Li$_{0.92}$Mg$_{4.08}$. It can be roughly denoted as reaction (9). The only difference from that which occurred in the MgH$_2$–LiAlH$_4$ system is the formation of Li$_3$Mg$_7$ phase.

$$MgH_2 + LiH_2 \rightarrow Li_{0.92}Mg_{4.08} + Li_3Mg_7 + H_2\uparrow \tag{9}$$

The product phases in MgH$_2$–LiH–Al (1:1:1) after dehydrogenation at 500 °C are Li$_{0.92}$Mg$_{4.08}$ and Mg$_{17}$Al$_{12}$, the same as that yielded in the MgH$_2$–LiAlH$_4$ system.

Fig. 6 exhibits the isothermal de/re-hydrogenation kinetics of the MgH$_2$–LiH (1:1) composite at 500 °C. The XRD pattern for the samples after re-hydrogenation in Fig. 7 reflects that MgH$_2$ and LiH can eventually be reformed. It demonstrates that the hydrogen storage in the MgH$_2$–LiH composite can be fully reversible.

3.3. De/re-hydrogenation kinetics of the MgH$_2$–LiAlH$_4$ system

Presently synthesized MgH$_2$–LiAlH$_4$ systems exhibit enhanced dehydrogenation kinetics. In Fig. 8, one can observe that their incubation time for decomposition was greatly reduced from pristine MgH$_2$. At around 400 °C, it takes only 200 s to start hydrogen desorption and another 400 s to reach saturation. This phenomenon
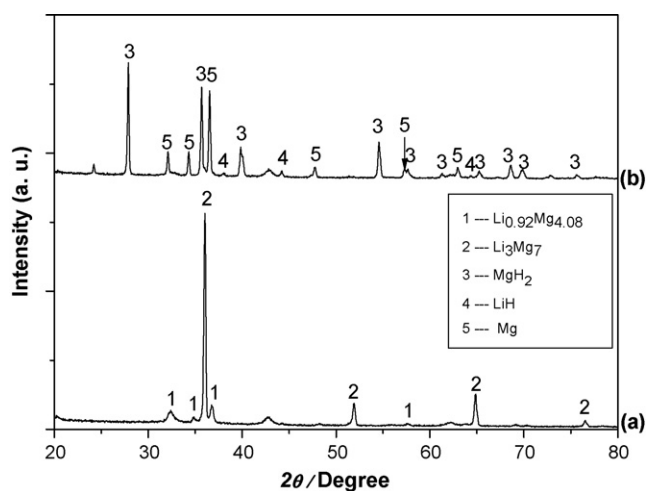

Fig. 8. Isothermal dehydrogenation kinetics for MgH$_2$–LiAlH$_4$ composites (in mole ratio of 1:1, 2:1 and 4:1) at 400 °C.

is different from previous reports that additional LiAlH$_4$ (5 at.%) hardly influenced the dehydrogenation kinetics of MgH$_2$ [30]. We speculate that sufficient amounts of LiAlH$_4$ in the composite are of fundamental importance to enhance the kinetics. Abundant doping of LiAlH$_4$ might result in a systematic reaction both on the surface and in the bulk of MgH$_2$, which will alter its activation energy of decomposition.

The activation energy of MgH$_2$-relevant decomposition in the MgH$_2$–LiAlH$_4$ (4:1) composite was estimated by means of Kissinger's method [31] using the following equation:

$$\ln\left(\frac{\beta}{T_p^2}\right) = -\frac{E_a}{RT_p} + \alpha \tag{9}$$

where β is the heating rate, T_p is the peak temperature, R is the gas constant, E_a is the activation energy for the dehydrogenation reaction, and α is the linear constant.

The inset of Fig. 9 shows Kissinger's plot of the dehydrogenation reaction for the MgH$_2$–LiAlH$_4$ (4:1) composite obtained from DSC traces measured at various heating rates (β = 2, 5, 10 and 20 °C min^{-1}, respectively). From the slope of the straight line, the activation energy of as-synthesized MgH$_2$ is estimated to be 191 kJ mol^{-1}, which is greatly reduced from the reported value of

Fig. 7. XRD patterns for the isothermal de/re-hydrogenated MgH$_2$–LiH composite (in mole ratio of 1:1) at 500 °C. (a) dehydrogenated sample; (b) rehydrogenated sample.

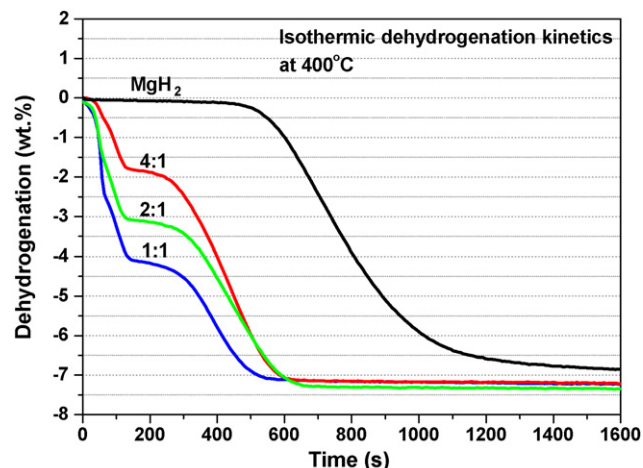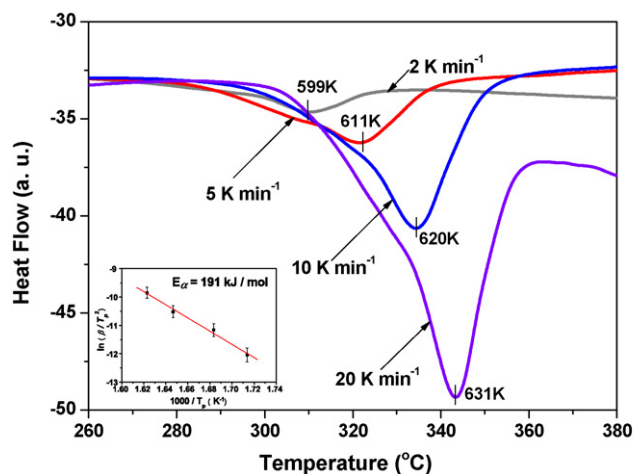**Fig. 9.** DSC traces measured at various heating rates (β = 2, 5, 10, 20 °C min^{-1}, respectively) for the MgH$_2$–LiAlH$_4$ (4:1) composite. The inset plot is achieved by Kissinger's method with the parameters obtained from the DSC measurements.
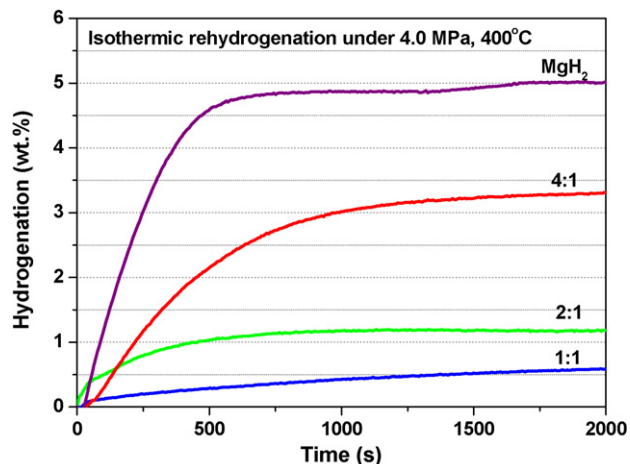
Fig. 10. Isothermal re-hydrogenation kinetics for MgH_2–$LiAlH_4$ composites (in mole ratio of 1:1, 2:1 and 4:1) at $400\,^\circ C$.

pristine MgH_2 $(323\,kJ\,mol^{-1})$ [32]. It can be suggested that the reaction with LiH and Al phases leads to a more activated surface of MgH_2. We further hypothesize that the subsequently formed $Li_{0.92}Mg_{4.08}$ and $Mg_{17}Al_{12}$ phases create a beneficial pathway for the hydrogen atoms diffusion to the surface and recombination. However, the pathway might be ineffective for re-hydrogenation. Because according to Fig. 10, the re-hydrogenation kinetics is greatly depressed with an increase of $LiAlH_4$ in the system.

4. Conclusions

In the present work, MgH_2 was effectively destabilized in an MgH_2–$LiAlH_4$ system. The onset dehydrogenation temperature of MgH_2 in the composites was observed at around $250\,^\circ C$, which is reduced significantly by more than $50\,^\circ C$ from that of as-milled pristine MgH_2. DSC measurements exhibit that the enthalpies of MgH_2-relevant decomposition in the composites (1:1, 2:1 and 4:1 in mole ratio) are 45, 48.6 and $61\,kJ\,mol^{-1}$ H_2, respectively. The values are significantly smaller than that of pristine MgH_2 $(76\,kJ\,mol^{-1}$ $H_2)$, demonstrating the destabilization of MgH_2 in this system.

XRD analyses indicate that the whole dehydrogenation process can be divided into two stages: The first stage belongs to the self-decomposition of $LiAlH_4$. At the second stage, the yielded LiH and Al phases decompose MgH_2 to form $Li_{0.92}Mg_{4.08}$ and $Mg_{17}Al_{12}$ phases, respectively. The mutual destabilization between MgH_2 and LiH was first observed in this case. When the thoroughly dehydrogenated system is reloaded by 4 MPa H_2, MgH_2 could be partially reversible but $LiAlH_4$ is irreversible.

An investigation of the isothermal kinetics for the MgH_2–$LiAlH_4$ system indicates that the doped $LiAlH_4$ is beneficial to the enhancement of dehydrogenation kinetics. The activation energy for the decomposition of MgH_2 in the MgH_2–$LiAlH_4$ (4:1) composite can be reduced to $191\,kJ\,mol^{-1}$. However, the yielded Mg_2Al_3 phases inhibit the re-hydrogenation of the MgH_2–$LiAlH_4$ system.

Acknowledgements

References

[1] L. Schlapbach, A. Züttel, Nature 414 (2001) 353–358.
[2] F. Schüth, B. Bogdanović, M. Felderhoff, Chem. Commun. 20 (2004) 2249–2258.
[3] P.-A. Huhn, M. Dornheim, T. Klassen, R. Bormann, J. Alloys Compd. 404–406 (2005) 499–502.
[4] A. Zaluska, L. Zaluski, J.O. Strom-Olson, J. Alloys Compd. 289 (1999) 197–206.
[5] G. Liang, J. Huot, S. Boily, A. Van Neste, R. Schulz, J. Alloys Compd. 291 (1999) 295–299.
[6] G. Liang, J. Huot, S. Boily, R. Schulz, J. Alloys Compd. 305 (2000) 239–245.
[7] C.X. Shang, M. Bououdina, Y. Song, Z.X. Guo, Int. J. Hydrogen Energy 29 (2004) 73–80.
[8] G. Liang, J. Huot, S. Boily, A. Van Neste, R. Schulz, J. Alloys Compd. 292 (1999) 247–252.
[9] G. Liang, J. Huot, S. Boily, A. Van Neste, R. Schulz, J. Alloys Compd. 297 (2000) 261–265.
[10] H. Gu, Y.F. Zhu, L.Q. Li, J. Alloys Compd. 424 (2006) 382–387.
[11] W. Oelerich, T. Klassen, R. Bormann, J. Alloys Compd. 315 (2001) 237–242.
[12] G. Barkhordarian, T. Klassen, R. Bormann, Scr. Mater. 49 (2003) 213–217.
[13] O. Friedrichs, T. Klassen, J.C. Sanchez-Lopez, R. Bormann, A. Fernandez, Scr. Mater. 54 (2006) 1293–1297.
[14] O. Friedrichs, F. Aguey-Zinsou, J.R. Fernandez, J.C. Sanchez-Lopez, A. Justo, T. Klassen, R. Bormann, A. Fernandez, Acta Mater. 54 (2006) 105–110.
[15] J.-L. Bobet, S. Desmoulins-Krawiec, E. Grigorova, F. Cansell, B. Chevalier, J. Alloys Compd. 351 (2003) 217–221.
[16] N. Hanada, T. Ichikawa, H. Fuji, J. Phys. Chem. B 109 (2005) 7188–7194.
[17] E. Ivanov, I. Konstanchuk, B. Bokhonov, V. Boldyre, J. Alloys Compd. 359 (2003) 320–325.
[18] J.F.R. de Castro, A.R. Yavari, A. LeMoulec, T.T. Ishikawa, W.J. Botta, J. Alloys Compd. 389 (2005) 270–274.
[19] A.R. Yavari, A. LeMoulec, J.F.R. de Castro, S. Deledda, O. Friedrichs, W.J. Botta, G. Vaughan, T. Klassen, A. Fernandez, A. Kvick, Scr. Mater. 52 (2005) 719–724.
[20] S. Deledda, A. Borissova, C. Poinsignon, W.J. Botta, M. Dornheim, T. Klassen, J. Alloys Compd. 404–406 (2005) 409–412.
[21] V.V. Bhat, A. Rougier, L. Aymard, X. Darok, G. Nazri, J.M. Tarascon, J. Power Sources 159 (2006) 107–110.
[22] L.-P. Ma, P. Wang, H.-M. Cheng, J. Alloys Compd. 432 (2007) 1–4.
[23] S.-A. Jin, J.-H. Shim, Y.W. Cho, K.-W. Yi, J. Power Sources 172 (2007) 859–862.
[24] J.J. Vajo, J. Phys. Chem. B 108 (2004) 13977–13983.
[25] J. Chen, N. Kriyama, Q. Xu, H.T. Takeshita, T. Sakai, J. Phys. Chem. B 105 (2001) 11214–11220.
[26] A. Zaluska, L. Zaluski, J.O. Ström-Olsen, Appl. Phys. A 72 (2001) 157–165.
[27] H. Yabe, T. Kuji, J. Alloys Compd. 433 (2007) 241–245.
[28] Q.A. Zhang, H.Y. Wu, Mater. Chem. Phys. 94 (2005) 69–72.
[29] J.R. Ares, K.-F. Aguey-Zinsou, M. Porcu, J.M. Sykes, M. Dornheim, T. Klassen, R. Bormann, Mater. Res. Bull. 43 (2008) 1263–1275.
[30] J. Huot, G. Liang, R. Schulz, J. Alloys Compd. 353 (2003) L12–L15.
[31] H.E. Kissinger, Anal. Chem. 29 (1957) 1702–1706.
[32] N. Hanada, T. Ichikawa, H. Fujii, J. Phys. Chem. B 109 (2005) 7188–7194.